ISSN 0016-7932, Geomagnetism and Aeronomy, 2016, Vol. 56, No. 5, pp. 557–571. © Pleiades Publishing, Ltd., 2016.
Original Russian Text © N.M. Polekh, N.A. Zolotukhina, E.B. Romanova, S.N. Ponomarchuk, V.I. Kurkin, A.V. Podlesnyi, 2016, published in Geomagnetizm i Aeronomiya, 2016, Vol. 56, No. 5, pp. 591–605.

Ionospheric Effects of Magnetospheric and Thermospheric Disturbances on March 17–19, 2015

N. M. Polekh*, N. A. Zolotukhina, E. B. Romanova***, S. N. Ponomarchuk****, V. I. Kurkin, and A. V. Podlesnyi**

Institute of Solar–Terrestrial Physics, Siberian Division, Russian Academy of Sciences, Irkutsk, 664033 Russia

**e-mail: polekh@iszf.irk.ru*
***e-mail: zolot@iszf.irk.ru*
****e-mail: ebr@iszf.irk.ru*
*****e-mail: spon@iszf.irk.ru*

Received August 19, 2015; in final form, December 23, 2015

Abstract—Using vertical and oblique radio-sounding data, we analyze the ionospheric and thermospheric disturbances during the magnetic storm that occurred in northeastern Russia on March 17–19, 2015. We consider the heliospheric sources that induced the magnetic storm. During the main and early recovery phases, the midlatitude stations are characterized by extremely low values of electron density at the *F*2 layer maximum. Using oblique sounding data, we recorded signals that propagated outside the great circle arc. In evening and night hours, no radio signals were found to pass along the Norilsk–Irkutsk and Magadan–Irkutsk paths. The observed ionospheric effects are shown to be caused by a sharp shift of the boundaries of the main ionospheric trough to the invariant latitude 46° N during the main phase of the magnetic storm. The negative ionospheric disturbance during the recovery phase of the storm, which was associated with significant variations in the composition of the neutral atmosphere, led to a change in the mode composition of received radio signals and a decline in observed maximal frequencies in daytime hours of March 18, 2015 by more than 2 times.

DOI: 10.1134/S0016793216040174

1. INTRODUCTION

Geomagnetic storms are known to cause a number of various phenomena in the ionosphere (ionospheric storms) that substantially change its parameters and thus the characteristics of the ionospheric radio channel. The intensity of ionospheric storms depends on energy arrival from the heliosphere to the external geospheres (magnetosphere, ionosphere, and thermosphere) and redistribution of energy between them. The study of these processes is one of the main problems of space geophysics, and there are many reviews and interesting studies addressing this topic, such as (Danilov and Belik, 1991; Prölss et al., 1991; Buonsanto, 1999; Danilov and Laštovička, 2001; Mendillo, 2006; Danilov 2013), which are based on ground-sensing data and satellite and navigation measurements. The ionospheric response to magnetic disturbances is shown possibly to differ significantly from one storm to another, and the level of ionospheric disturbances even during the same storm varies at different latitudes (Danilov, 2013).

The properties of the ionospheric radio channel of high-frequency (HF) radio paths depend on the location of transmitting and receiving stations, the length and orientation of paths, and the level of geomagnetic disturbances. An analysis of the parameters of received HF radio signals on polar and subauroral paths indicated that the nonuniform structure of the high-latitude ionosphere leads to the fact that the modal composition of these signals becomes complex (comprising not only multihop modes but also combined modes with a mixed reflection from the *E*- and *F*-regions (Evlashina et al., 1986; Blagoveshchenskii and Zherebtsov, 1987; Warrington et al., 2006). An increase in geomagnetic activity is accompanied by shifted boundaries of the main ionospheric trough (MIT) and the zone of particle precipitation to the equator, increased gradients of electron density at their boundaries, and a changed time of radio signal propagation, which substantially changes the propagation characteristics of HF radiowaves. During magnetic storms, the oblique sounding ionograms obtained along subauroral paths record extra diffuse signals propagating outside the great circle arc (Blagoveshchenskii and Zherebtsov, 1987; Zherebtsov et al., 1997; Blagoveshchensky and Borisova, 2000; Kurkin et al., 2006.; Warrington et al., 2006). The maximum observed frequencies (MOFs) of these signals often exceed the MOFs of standard propagation modes. According to

trajectory calculations conducted by Mingalev et al. (1990), the formation of large-scale nonuniformities in electron density along the propagation path can lead to the disappearance of high-multiplicity modes and even to the complete absence of received radio signals.

The set of heliogeophysical phenomena observed on March 16–19, 2015, led to the development of a large magnetic storm with effects manifested in significant variations in the ionospheric and thermosphere and in the characteristics of HF radiowaves along subauroral and midlatitude paths.

In this paper, we aim to conduct a comprehensive study of variations in ionospheric and thermospheric parameters at middle and subauroral latitudes during the main and recovery phases of the magnetic storm of March 17–19, 2015. To this end, we consider heliospheric and magnetospheric disturbances on the basis of satellite and ground-based observation data (Section 2). Based on vertical-incidence ionosonde data and data of the network of three radio paths located in northeastern Russia, we investigate the variations in ionospheric parameters (Section 3) and the propagation characteristics of HF radiowaves (Section 4). Section 5 discusses of the experimental data and the results of simulations of the electron density distribution in the ionosphere taking into account the specific conditions of this storm. The main results are presented in the Conclusions.

2. GEOMAGNETIC DISTURBANCES AND THEIR HELIOSPHERIC SOURCES

The plot of the change in the *Dst*-index (http://wdc.kugi.kyoto-u.ac.jp/dst_provisional/201503/index.html) shows that 0400–0500 UT on March 17, 2015, was the onset time of a strong magnetic storm that terminated on March 25, 2015, after 1200 UT. At the storm maximum, which was observed at 2200–2300 UT on March 17, the *Dst*-index decreases to –223 nT. According to the information at (http://www.solen.info/ solar/old_reports/) based on the SOHO satellite data, this storm developed during the interaction of the Earth's magnetosphere with high-speed heliospheric plasma flows associated with four coronal holes and the emission accompanying the X-ray flare of class C9.1 that was registered at 0115–0213 UT on March 15, 2015.

More detailed data on changes in the ring current field during the first three days of the magnetic storm are given from the plot of changes in the *SYM-H*-index, shown together with plots of the *Kp*- and *AE*-indices in Fig. 1. The geomagnetic activity indices were taken from (http://wdc.kugi.kyoto-u.ac.jp). The plot of *SYM-H* clearly shows the storm sudden commencement (SSC). The initial phase of the storm with *SYM-H* = 46–67 nT lasted around 1.5 h. The next 16.5 h show a slow decrease in *SYM-H* down to its minimum of –234 nT reached at 2247 UT. Based on *SYM-H* variations, one can specify the intervals of different phases of the magnetic storm:

0445–0622 UT on March 17, 2015 (initial phase);

0623–2247–2306 UT on March 17, 2015 (main phase and storm maximum);

2307–0016 UT on March 17–18, 2015 (early recovery phase);

0017–1757 UT on March 18, 2015 (part of late recovery phase).

Figure 1 marks the boundaries of these intervals by vertical dotted lines A–E. In the initial phase of the storm, the planetary geomagnetic *Kp*-index sharply increased from 2 to 5. The auroral activity (the *AE*-index) remained almost unchanged. The short-term increase in the *AE*-index from 52 nT at 0445 UT to 269 nT at 0447 UT was observed only during the SSC; however, the average values of *AE* remained at the level of ≤100 nT until 0606 UT.

The auroral activity started to gradually increase after 0600 UT, i.e., approximately 20 min before the main phase of the storm. During the main and early recovery phases, the *Kp*-index varied nonmonotonically from 5+ to 8– and the *AE*-index varied from 65 to 2300 nT. When turning to the late recovery phase (after 0017 UT on March 18, 2015), the auroral activity weakened. During the next 8 h, the *AE*-index was lower than 400 nT.

The variations in the solar wind parameters—*Bz*- and *By*-components of the interplanetary magnetic field (IMF)—for March 17–18, 2015, are shown in Figs. 2a and 2b. These figures are based on the ACE satellite data taken from (ftp://ftp.swpc.noaa.gov/pub/warehouse). The vertical dotted lines A–E mark the heliospheric plasma boundaries corresponding to the aforementioned different phases of the magnetic storm. After 0406 UT of March 17, 2015, there are strong fluctuations in th evelocity (*Vsw*) and density (*Nsw*) of the solar wind the and *By*- and *Bz*-components of the IMF. It can be seen that each (even a relatively weak) change in the aforementioned parameters can trigger substorm-type geomagnetic disturbances and become a factor that enhances the diffusion of plasma layer particles and solar cosmic rays into the inner magnetosphere (Lyons and Williams, 1987).

It is known that the main factor controlling the structure of the magnetosphere and the development of the ring current is the field of magnetospheric convection (Gonzalez et al., 2002). The variations in the magnetospheric convection field (*Ec*), as calculated according to ACE satellite data with the formulas described in (Burke et al., 2007), are shown in Fig. 2c (upper plot). Each point of the plot of *Ec* is shifted along the time axis by $\Delta UT = (X_{GS} - Rmag)/Vsw$ (the

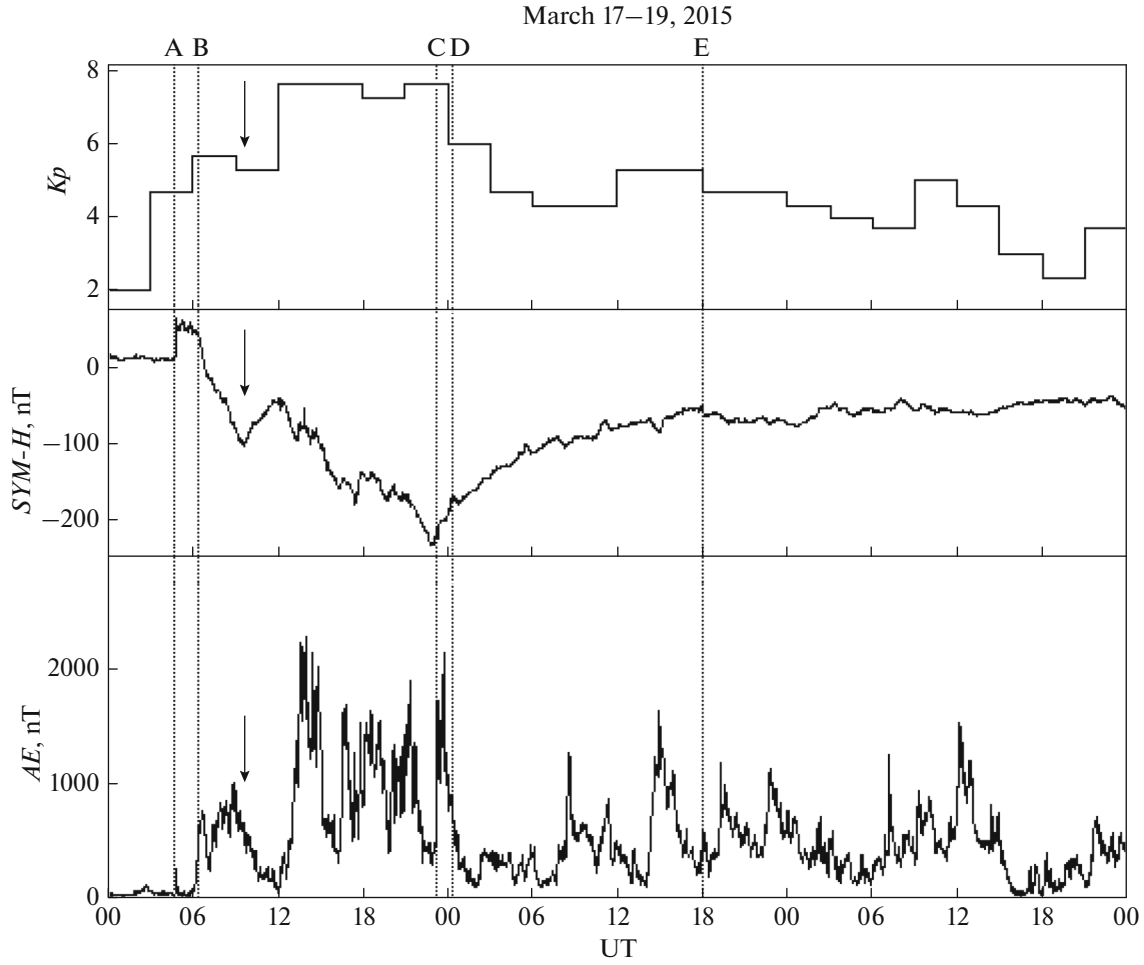

Fig. 1. Variations in *Kp*- (top panel), *SYM-H*- (middle panel), and *AE*- (bottom panel) indices. In this and subsequent figures, the vertical dotted lines denote: (A) SSC; (B) beginning of the main phase, (C) early recovery phase, (D) late recovery phase, and (E) end of the interval of relatively stable growth in the *SYM-H*-index. The arrows denote the first minimum of *SYM-H*.

time of propagation of the given fragment of heliospheric plasma to the magnetosphere).

Comparing the variations in *Ec* with variations in heliospheric parameters (*AU*- and *AL*-indexes), one can see that the first significant increase in *Ec* up to ~1.2 mV/m at around 0600 UT on March 17, 2015, corresponds (by time) to the interval of the southward *Bz*-component of the IMF. The decrease in *Bz* to –20 nT was accompanied by an increase in the *AU*-index and a decrease in the *AL*-index by 400–450 nT, i.e., by an enhanced two-vortex current system of magnetospheric convection. The following longer increase in *Ec* of up to 1 mV/m also corresponded to a decrease in *Bz* to –20 nT. In this case, the *AL*-index decreased to its minimum (–914 nT at 0852 UT on March 17, 2015). The *AU*-index decreased to 1–113 nT. And, finally, the longest 12-h increase in *Ec* at 1200–2400 UT to 0.6–1.5 mV/m coincided (by time) with a prolonged increase of the western electrojet in the auroral region, when the *AL*-index decreased repeatedly to –1000 nT. It should be noted that the early recovery phase of the storm developed on the background of *Ec* decreasing from 0.8 to 0.55 mV/m and negative magnetic bays in the auroral zone; in the phase of their enhancement from 2313 to 2315 UT, the *AL*-index sharply decreased from –450 to –1670 nT.

3. IONOSPHERIC DISTURBANCES IN NORTHEASTERN ASIA ACCORDING TO VERTICAL SOUNDING DATA

The ionospheric disturbances caused by magnetic storms were analyzed with the use of ionograms of vertical-incidence sounding at the Yakutsk (62.0° N, 129.6° E), Mohe (52.0° N, 122.5° E), Tunguska (61.6° N, 90.0° E), Magadan (60.0° N, 151.0° E) (http://ulcar.uml.edu/DIDBase/, http://space-weather.ru), and Irkutsk (52.5° N, 104° E) stations. The ionograms have a standard resolution of 15 min, except for Mohe station (5-min resolution). In addition, 1-min data

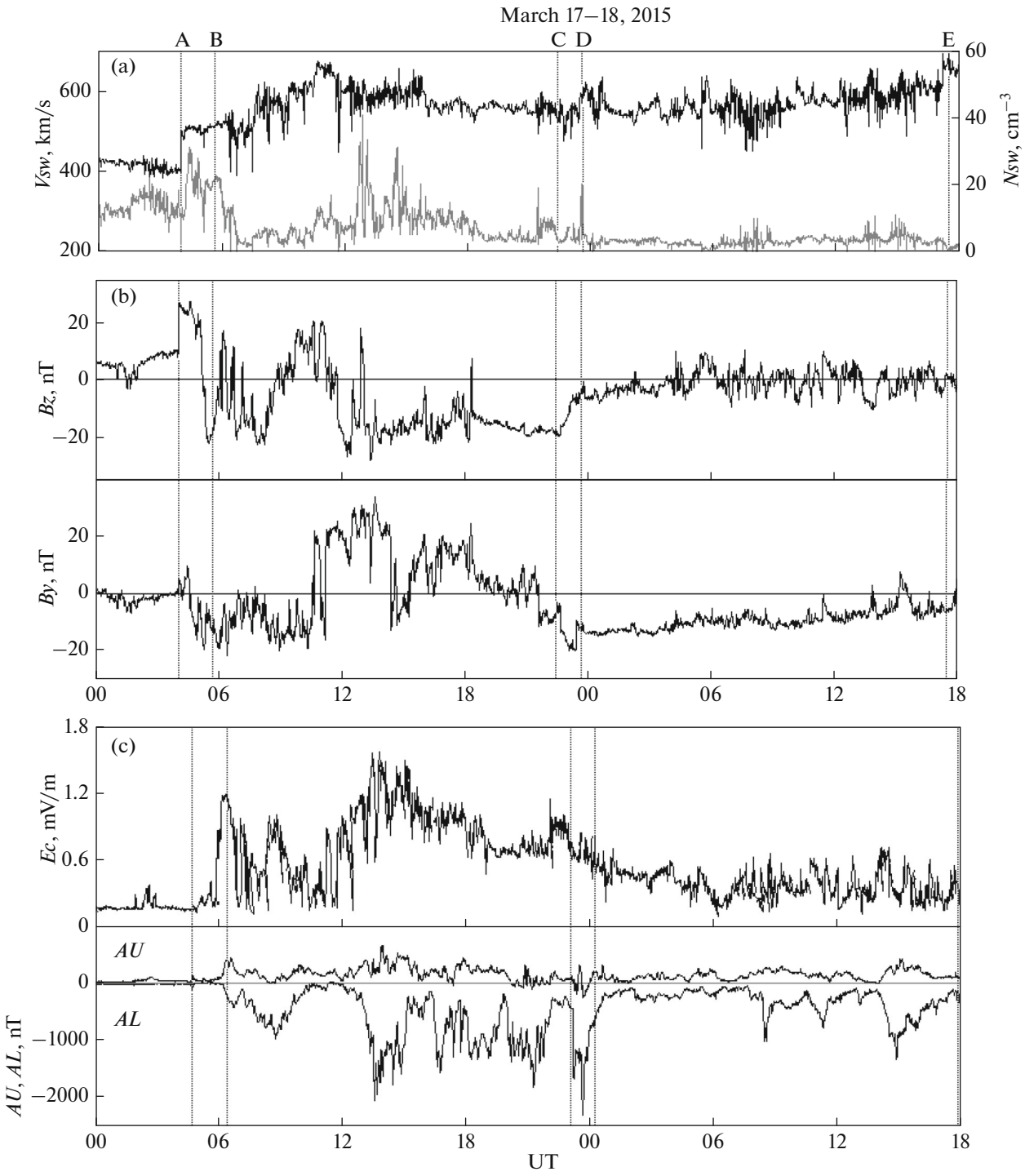

Fig. 2. (a) Temporal evolution of solar wind speed (black line) and density (gray line); (b) variations in *Bz*- and *By*-components of the IMF; and (c) changes in the magnetospheric convection field compared with variations in *AU*- and *AL*-indices.

from vertical-incidence and low-incidence ionosondes located 124 km away from Irkutsk were used. The changes in critical frequencies (*foF*2), electron density peak height (*hmF*2), and minimum virtual height of reflections from the *F*-region (*h'F*) were estimated with respect to background values calculated as an average of the analyzed parameters for March 13–14, 2015 (days of low geomagnetic activity).

Figure 3 shows the variations in critical frequencies at these stations recorded on March 17–19, 2015. At the Yakutsk station at the beginning of the main phase of the storm, *foF*2 decreased relative to background

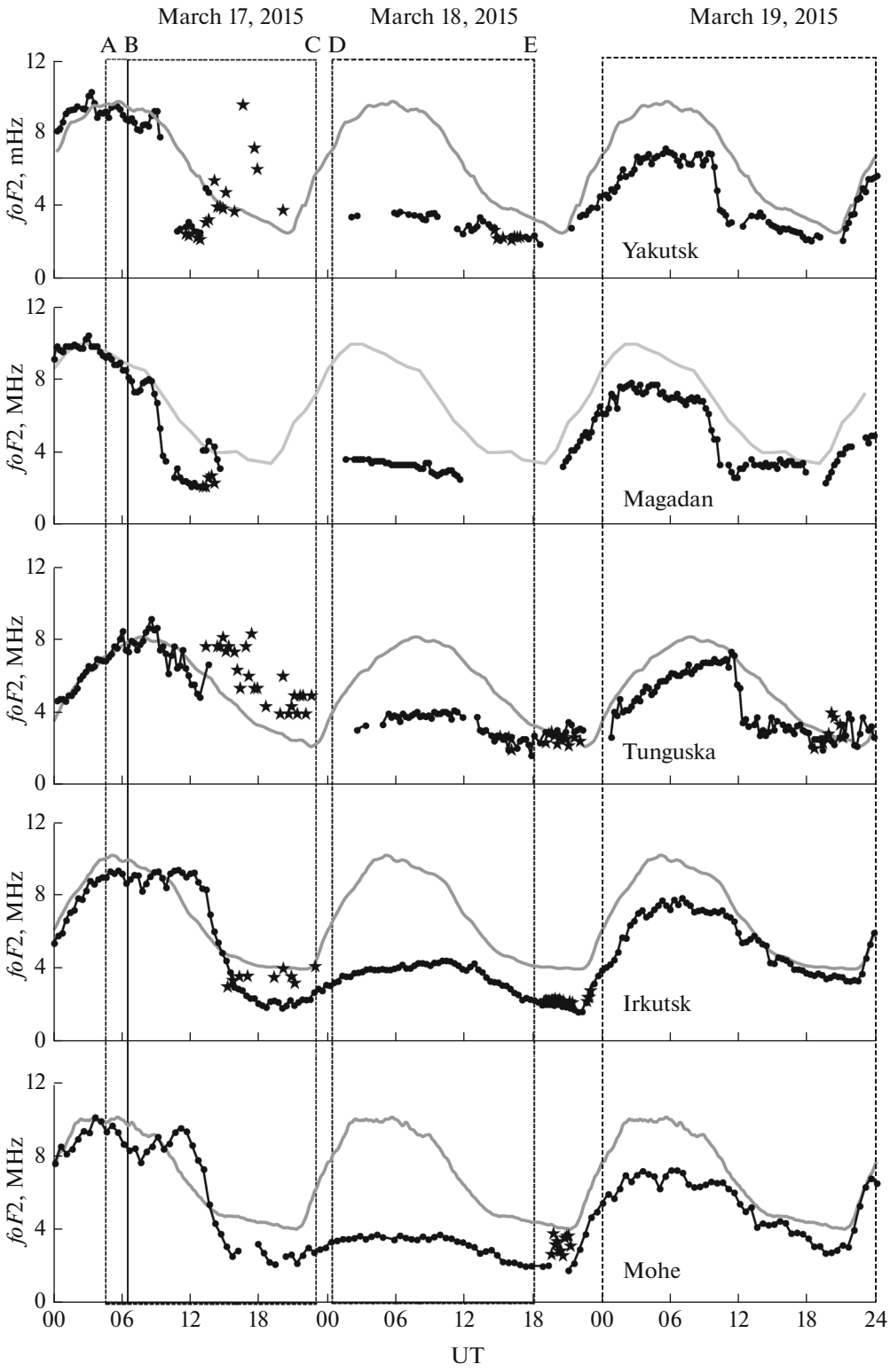

Fig. 3. Variations in critical frequencies at some ionospheric stations on March 17–19, 2015: background values (gray line), current values (black line), and *foEs* (asterisks).

values. The *foF*2 oscillations observed in the background of its decrease can be associated with increased activity of propagating ionospheric disturbances. The changes in *foF*2 were the most considerable after 0900 UT, when the *Bz*-component of the IMF decreased to –20 nT and the convection field intensified. At 0915 UT, diffuse signals were recorded. The tracks on ionograms then disappeared up to 1030 UT.

From this time to 1200 UT, reflections with critical frequencies not exceeding 2.2–2.7 MHz, which were typical for the MIT, were recorded. The reflections from the *F*2-layer were accompanied by weak signals from the *E*-region (from 1115 UT) and lateral diffuse signals reflected from the polar MIT wall. The ionograms included a clear shift of these diffuse signals with time to lower heights. From 1300 UT, the Yakutsk station was in the diffuse precipitation zone: the lateral reflections disappeared, and the scattered signals from the *F*2-layer (*foF*2 ~ 4.0–4.5 MHz) were accompanied by sporadic layers (*Es*) with limited frequencies of up to 5 MHz. From 1345 UT to the end of March 17, 2015, only sporadic blanketing layers alternating with complete absorption sessions were observed.

At the beginning of the main phase of the magnetic storm, the time course of critical frequencies in Magadan was similar to the variations in *foF*2 in Yakutsk. In the background of a general reduction of critical frequencies from 0915 to 0945 UT, lateral scattered reflections with frequencies of up to 6–9 MHz were recorded. Then, until 1030 UT, no reflections were present. From 1030 to 1300 UT, there were simultaneously recorded reflections from the *F*2-layer with low values of *foF*2 (typical for the MIT) and lateral scattered signals. From 1315 to 1400 UT, the ionograms had simultaneously diffuse reflections from the *F*2-layer with frequencies of 3.8–4.5 MHz and sporadic layers from blanketing frequencies of 2.5–2.8 MHz. After 1400 UT, the reflections from the *E*-region disappeared first and, after 1430 UT, the reflections from the *F*-region disappeared.

At the beginning of the main phase in Tunguska, oscillations of *foF*2 were recorded. From 1000 UT, scattered signals from the *F*-region recorded; from 1245 to 1300 UT, scattered signals from the *E*- and *F*-regions were recorded. From 1315 to 2200 UT, only blanketing *Es* were recorded.

A specific feature of *foF*2 variations at midlatitude stations of Irkutsk and Mohe is the formation of positive disturbances in the evening hours of local time (LT) on March 17, 2015. At the Mohe and Irkutsk stations, the *foF*2 values increased relative to background values by 30–44% from 1117 to 1242 UT and by 25–33% from 1145 to 1315 UT, respectively. This increase in *foF*2 can be explained by intensified equatorward meridional wind and, as a consequence, by increased vertical upward drift velocity. The results of calculations performed with the model (Drob et al., 2008) indicated that, after 0500 UT at Mohe and after 0600 UT at Irkutsk, the vertical drift velocity increased to 38 and 32 m/s, respectively (Fig. 4a). In view of the complex structure of ionograms recorded during the disturbances, the height of the *F*2-layer maximum cannot be easily determined. Therefore, the analysis also involved the minimum virtual height of reflections from the *F*-region. The variations in *hmF*2 and *h'F* and in the diurnal course are similar. For example, for March 17, 2015 from 0000 to 1500 UT, the coefficient of correlation between them was 0.79; therefore, it can be assumed that the deviation of current values *h'F* from background values ($\Delta h'F$) can serve to assess the dynamics of the *F*-layer height in general. From 0925 to 1000 UT at Mohe and from 0945 to 1000 UT at Irkutsk, there was an increase in the peak height of electron density of the *F*2-layer by 35–65 km relative to the quiet level (Fig. 4b).

The layer height changes at these stations were most considerable after 1430 UT. Within a few minutes, the height abruptly increases by 70–90 km. The increases of *hmF*2 and *h'F* were recorded in the 2 h after the region with a southward *Bz*-component of the IMF comes to the subsolar magnetosphere. At the forefront of this region, the values of *Bz* sharply (within 3 min) changed from 4.3 to −11.9 nT. The values $Bz < -10$ nT were observed on the ACE satellite almost continuously from 1149 to 2307 UT. This region affected the Earth's magnetosphere nearly from 1230 to 2350 UT on March 17, 2015, and stimulated the growth in geomagnetic activity (*Kp*- and *AE*-indices) up to the maximum level (see Fig. 1).

In the background of enhanced geomagnetic activity in evening and night hours of local time, the midlatitude vertical sounding stations recorded extremely low values of *foF*2; for example, 2.13–2.3 MHz (1915–1935 UT) at Mohe and 1.8–2.01 MHz (1738–2105 UT) at Irkutsk. Together with the large values of *hmF*2 (~400–420 km), this confirms the fact that these stations were located in the MIT region. It should be noted that the *Es* values recorded by a 1-min resolution ionosonde in the evening and night hours (1515–2283 UT) had a limited frequency of ~2.2–2.4 MHz. At Mohe station from 1625 to 1740 UT and 1930 to 2005 UT, the ionograms had no reflections. Figure 4c shows the energy fluxes of precipitating electrons for these stations calculated with the the model (Hardy et al., 1987). This figure qualitatively explains the appearance of sporadic layers and the short-term absence of reflections on ionograms due to absorption.

During the recovery phase of the storm (March 18, 2015), the critical frequencies recorded at all stations considered here in morning and afternoon hours were lower than 4 MHz; sometimes, only reflections from the *F1*-layer (condition *G*) were observed. This condition was recorded from 0515 to 0915 UT (1115–1515 LT) at Tunguska and from 2310 to 0245 UT (0710–1045 LT) and from 0435 to 0515 UT (1235–1315 LT) at Mohe. At Yakutsk and Magadan, the daytime reflections from the *F*-region were extremely irregular. During night hours, the Magadan, Yakutsk, and Tunguska stations recorded *Es*-layers and diffuse reflections from the *F*-region. From night onward, the Irkutsk and Mohe stations the values of *foF*2 remained

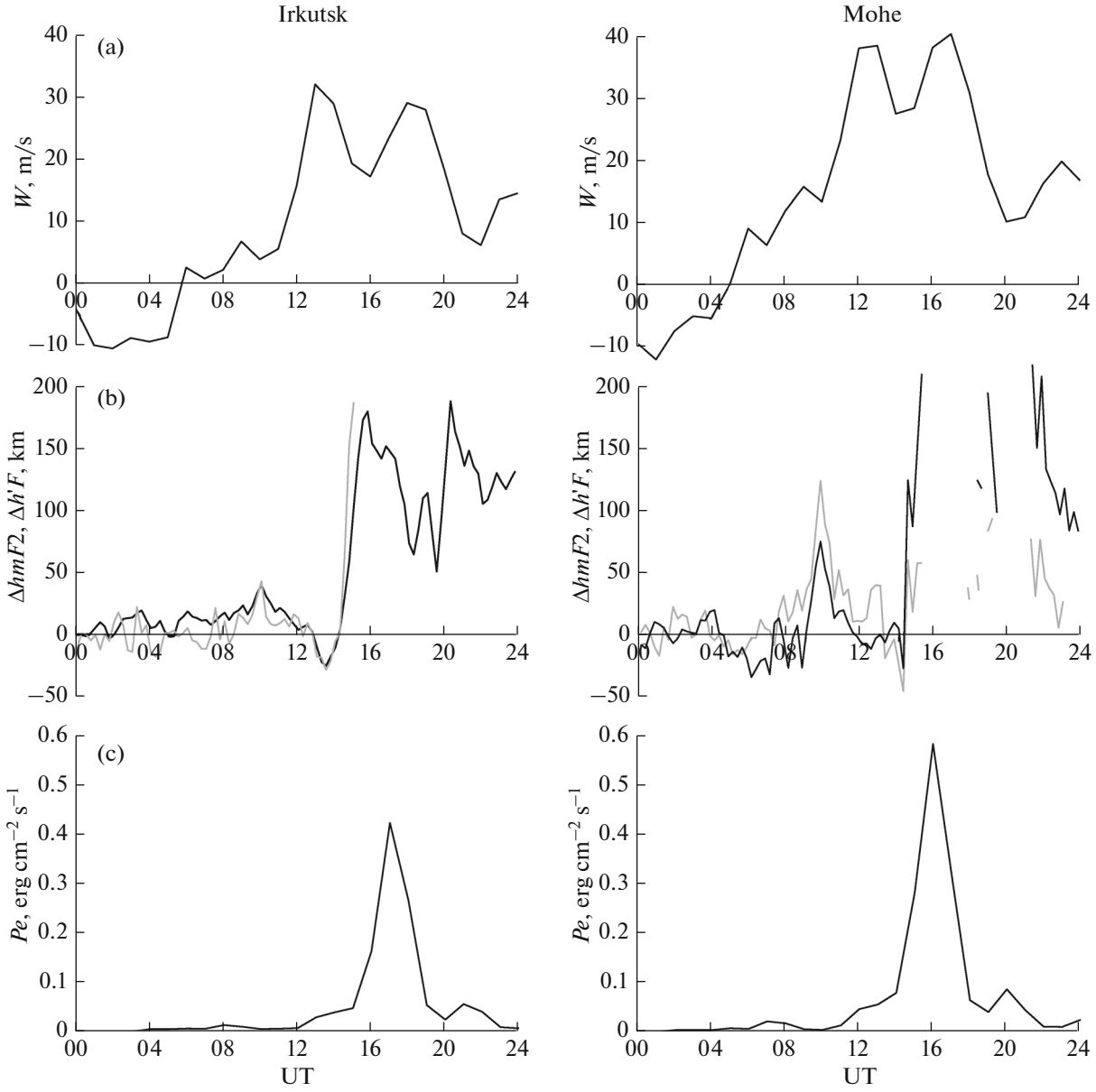

Fig. 4. (a) Variations in vertical drift velocity, (b) changes in $\Delta hmF2$ (gray line) and $\Delta h'F$ (black line), and (c) energy flux of precipitating electrons calculated for Irkutsk and Mohe conditions on March 17, 2015.

low ~1.9–2.1 MHz; in the early morning hours, sporadic layers were observed. At Mohe, they were recorded from 1935 to 2055 UT.

The next day (March 19, 2015) was characterized by a slow recovery of electron density, but the observed values of *foF*2 were significantly lower the background values; in evening hours at Yakutsk and Tunguska, there was a sharp decline. At Magadan, this decline is less clearly expressed. This means that the boundary of equatorial MIT wall recovered incompletely to the undisturbed state. At midlatitude stations, the nighttime *foF*2 values were likewise lower than the background values. As mentioned in Section 2, in the following days, the *Kp*-index increased up to 4 (March 21, 2015) and 6+ (March 22, 2015); therefore, the ionospheric parameters recover to the undisturbed level only after March 25, 2015.

4. MAGNETIC STORM EFFECTS ON VARIATIONS IN HF RADIOWAVES

The change in the parameters of HF radiowave propagation was analyzed with the use of data of three radio paths located in northeastern Russia: Magadan–

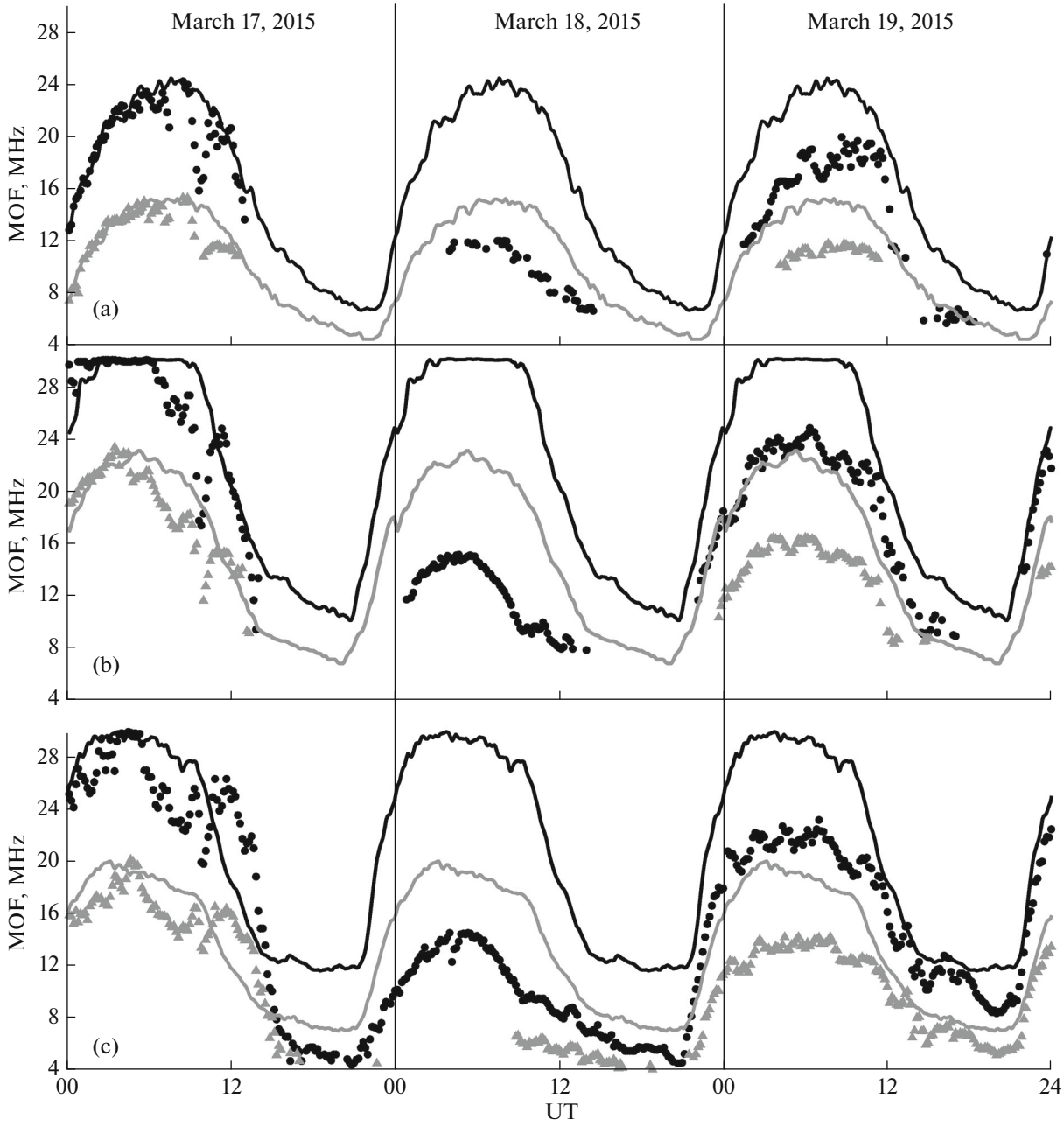

Fig. 5. Variations in MOFs along (a) Norilsk–Irkutsk, (b) Magadan–Irkutsk, and (c) Khabarovsk–Irkutsk paths. Background values of MOF mode 1*F* (black line), mode 2*F* (gray line), current values of MOF1*F* (black circles), and MOF2*F* (triangles).

Irkutsk (3034 km in distance), Khabarovsk–Irkutsk (2297 km in distance), and Norilsk–Irkutsk (2030 km in distance). The coordinates of the middle points of radio paths are (58.5° N, 125.8° E), (51.25° N, 119.6° E), and (60.9° N, 98° E), respectively. These paths were probed with an interval of 5 min. The two-way radio stations were equipped with linear FM-ionosondes operating in the frequency range of 4–30 MHz (Ivanov et al., 2003). In quiet geomagnetic conditions, the Magadan–Irkutsk path passes south of the MIT boundary; therefore, its position does not significantly affect the propagation characteristics of HF radiowaves, and the Khabarovsk–Irkutsk path is entirely located at middle latitudes.

Figure 5 shows the variations in the MOF of one-hop (1*F*) and two-hop (2*F*) modes for March 17–19, 2015, and the background values determined from data for March 13–14, 2015. In quiet geomagnetic conditions, the paths during daytime hours had multiple reflection modes (Figs. 6a and 6b). The beginning of the main phase of the storm was accompanied by traveling ionospheric disturbances causing MOF oscil-

lations along all paths in the background of their reduction. This manifested itself on oblique-sounding ionograms as individual "hooks" and "bends" (Figs. 6c and 6d). Starting with 0858 UT, the Magadan–Irkutsk and Norilsk–Irkutsk paths had more diffuse signals (denoted as mode 1*X* in Figs. 6e and 6f). These signals are caused by reflection from the polar trough wall. As the trough boundaries move toward the path midpoint, the time of propagation of these signals decreased (Figs. 6g and 6h) to become close to the time of propagation of standard signals. Such signals propagating beyond the great circle arc were recorded previously over this path during magnetic disturbances (Zherebtsov et al., 1997; Kurkin et al., 2006).

After the sharp MOF decrease recorded on all paths at 0935–1010 UT in the afternoon hours of LT, the MOFs began to increase. A maximum increase with respect to previous values was observed at 1040–1200 UT over the Norilsk–Irkutsk path, at 1040–1124 UT along the Magadan–Irkutsk path, and at 1024–1209 UT over the Khabarovsk–Irkutsk path.

Starting with 1300 UT, the Norilsk–Irkutsk path lost the reflections of the 2*F* and then the 1*F* modes. This is conditioned by absorption in the lower ionosphere because sporadic screening layers were observed near the midpoint (Tunguska station) from this time to the end of the day. Over the Magadan–Irkutsk path, the 2*F* and 1*F* modes disappeared after 1310 UT and 1350 UT, respectively. At night, continuous reflected signals of the one-hop mode were recorded only along the Khabarovsk–Irkutsk path, but the MOF values were almost twice as small as the background values.

The afternoon hours in the next day were characterized by low MOF values: along all paths, their values declined by more than two times. The radio signals passed mostly with the one-hop mode. Only over the Khabarovsk–Irkutsk path, the afternoon hours has reflections of the one-hop and two-hop modes. At night, the reflected signals were observed only along the Khabarovsk–Irkutsk path. At the recovery phase on March 19, 2015, the daytime MOF values increased relative to the previous day and two-hop signals appeared over all paths. In evening and night hours, the Norilsk–Irkutsk and Magadan–Irkutsk paths had no reflections recorded on ionograms.

5. DISCUSSION OF RESULTS

Oblique and vertical sounding data can be used to identify the main ionospheric and thermospheric effects of the magnetic storm on Match 17–19, 2015 observed in northeastern Russia.

The first of these effects is associated with a sharp decrease in electron density for 1.5 h at Yakutsk and Magadan stations and in MOF over Norilsk–Irkutsk and Magadan–Irkutsk paths in the beginning of the main phase of the storm (0935–1010 UT). It can be assumed that this decrease in the electron density at subauroral latitudes was caused by significant variations in the *Bz*-component of the IMF (0630–1000 UT), which are associated with a rapid change in the field of magnetospheric convection *Ec* and the increased auroral activity at the beginning of the main phase of the storm. This shifted the trough boundaries in evening hours of local time to latitudes between 58°N and 60°N. According to vertical sounding data, extremely low values of *foF*2 (typical for the MIT) were recorded at Yakutsk from 1045 to 1230 UT (1945–2130 LT) and at Magadan from 1030–1145 UT (2030–2145 LT). At Tunguska, no such low values of *foF*2 were observed, because the shift in the boundary of diffuse precipitations began under conditions of sufficient illumination. In view of the simultaneous increase in electron density in the *E*- and *F*-layers due to particle precipitation, it can be noted that the boundary of diffuse precipitations was recorded at 1245 UT (1845 LT) at Tunguska, at 1300 UT (2200 LT) at Yakutsk, and at 1315 UT (2315 LT) at Magadan. As was shown earlier (Hajkowicz and Hunsucker, 1987; Prölss and Ocko, 2000), the heating of ionospheric plasma at high latitudes due to the electric field of magnetospheric convection and precipitation of particles leads to the generation of large-scale moving disturbances that propagate over long distances. These disturbances manifest themselves very clearly along the oblique sounding paths (Polekh et al., 2010). In addition, the plasma heating causes an increase in the equatorward meridional wind velocity and a growth in the upward vertical drift. The combined effect of these processes can explain the MOF increase up to 23–24 MHz (1045–1200 UT) over the Magadan–Irkutsk path, up to 21–22 MHz (1027–1152 UT) along the Norilsk–Irkutsk path, and up to 25–26 MHz (1045–1200 UT) over the Khabarovsk–Irkutsk path. This positive disturbance was recorded at stations of vertical sounding in Irkutsk and Mohe (1030–1145 UT). The mechanism of the generation of positive disturbances is described in detail in (Danilov and Belik, 1991; Buonsanto, 1999), and elsewhere. The model calculations of the vertical drift velocity (Fig. 4a) confirm this assumption.

The next effect of the magnetic storm manifested itself by the fact that the ionospheric phenomena typical for the subauroral ionosphere were recorded at midlatitudes. These phenomena involve an extremely low electron density with typical tracks on vertical sounding ionograms, additional diffuse incident signals appearing due to the reflection from inhomogeneities of the polar trough wall, and sporadic layers of the *E*- and *F*-regions caused by particle precipitation. At the end of the main phase of the storm, extremely low values of *foF*2 were observed at 1730–2215 UT (0030–0515 LT) at Irkutsk and at 1915–2045 UT (0315–0445 LT) at Mohe. Almost the same informa-

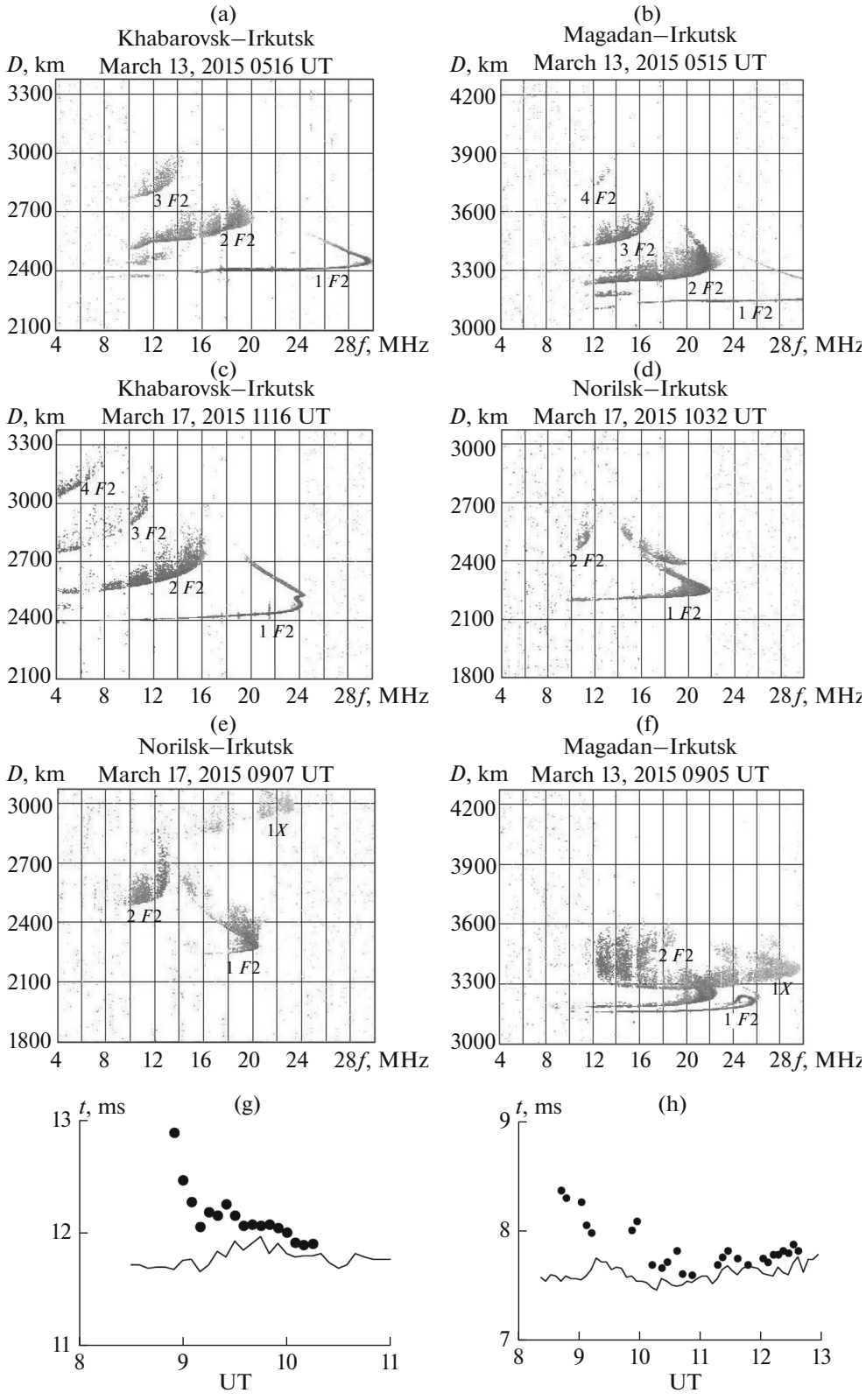

Fig. 6. Oblique sounding ionograms: (a, b) recorded in quiet geomagnetic conditions, (c, d) illustrating the emergence of shifting ionospheric disturbances, and (e, f) with recording of signals propagating beyond the great circle arc. (g, h) Variations in the time of propagation of additional signals (mode 1*X*) over the Norilsk–Irkutsk and Magadan–Irkutsk paths.

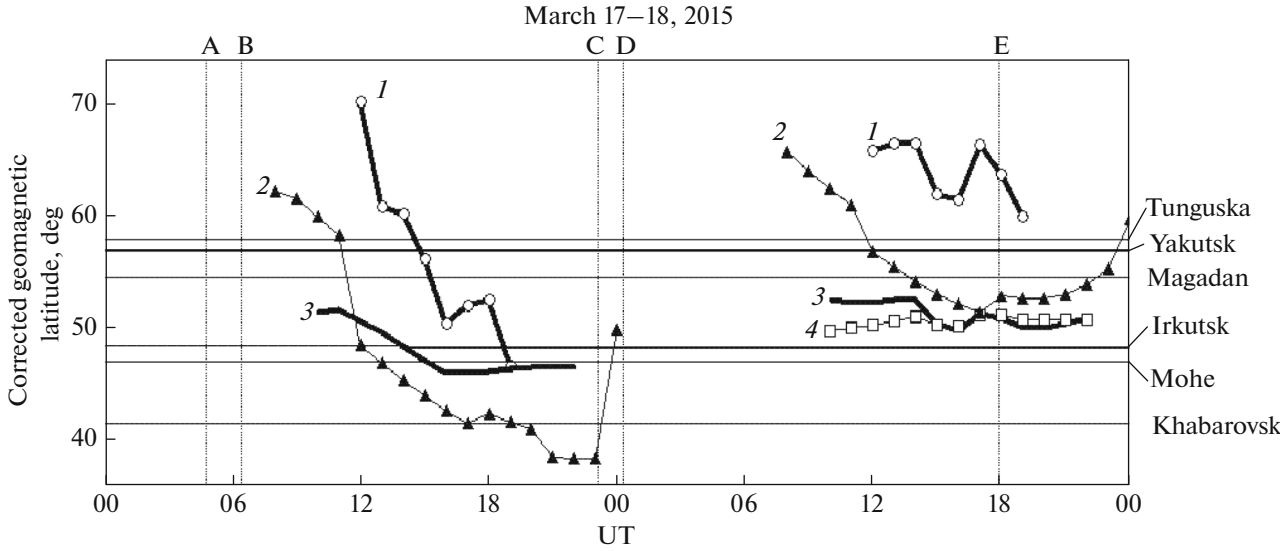

Fig. 7. Variations in the corrected geomagnetic latitude of electron precipitation boundary (*1*), minimum of the main (*2*, *3*), ring (*4*), and ionospheric troughs on the meridian 120° E according to calculations conducted by models: (*1*) (Kamide and Winningham, 1977); (*2*) (Zherebtsov et al., 1986), (*3*) (Deminov et al., 1996a), and (*4*) (Deminov et al., 1996b). The horizontal lines denote the corrected geomagnetic latitude of ionospheric stations.

tion about the dynamics of main structures was obtained from oblique sounding data. The MIT boundary shift can be explained by the prolonged existence of the negative *Bz*-component of the IMF after 1200 UT and the intensified field of magnetospheric convection.

We estimated the boundaries of main plasma structures for conditions of the given storm. By the current understanding of the magnetospheric structure, the nonmonotonic variations in *Vsw* and the *By*- and *Bz*-components of the IMF shown in Fig. 2 should have caused changes in the shape and position of the daytime magnetopause and the inner edge of the plasma sheet. Figure 7 shows the change in the boundaries of main plasma structures for March 17–18, 2015, as calculated from empirical models mostly for night hours. The model (Kamide and Winningham, 1977) calculated the position of the inner edge of the plasma sheet in the sector 2000–0400 MLT, which coincides with the boundary of diffuse precipitations, on the basis of the average value of the *Bz*-component of the IMF in the previous hour. The model (Zherebtsov et al., 1986) determines the latitude of the MIT minimum in the sector 1600–0800 MLT on the basis of current values of the *Kp*-index. The input parameters of the model determining the position of the MIT minimum by the model (Deminov et al., 1996a; Deminov et al., 1996b) are the average value of the *Kp*-index for the current and previous 4 h (the initial and main phases of the storm) and the ring current field (the recovery phase of the storm). According to the calculations (Fig. 7), the MIT boundary by the end of the main phase of the magnetic storm shifted to the invariant latitude 46°; i.e.; Irkutsk and Mohe were in the MIT zone. According to the calculations performed by the model (Kamide and Winningham, 1977), the zone of diffuse precipitations shifted to the invariant latitude 47°, which points to the existence of sharp gradients of electron density in the MIT polar wall. The possibility that the boundary of diffuse precipitations and MIT minimum can be close was indicated by Karpachev and Afonin (2004) in their study of the dynamics of boundaries of morphological structures of the high-latitude ionosphere during magnetic storm of March 22–23, 1979, according to *Kosmos 900* and *Interkosmos 19* satellite data. This conclusion is confirmed by spectrometric measurements performed at the geophysical observatory of the Institute of Solar–Terrestrial Physics, Siberian Division, Russian Academy of Sciences (51° N, 103° E). According to these data, the intensity of 630 nm emissions recorded on March 17, 2015, exceeded by 10 times or more the intensity of emissions recorded under quiet geomagnetic conditions (Beletskii et al., 2015).

The MIT position determined by empirical models corresponds to the electron density distribution maps obtained with the help of a mathematical model of the ionosphere (Tashchilin and Romanova, 2014). This model incorporates photoionization by the flux of solar ultraviolet radiation and by fluxes of precipitating particles, recombination through elastic and inelastic collisions, and the transfer of ionospheric plasma due to neutral winds and the electric field of magnetospheric convection. The parameters of the

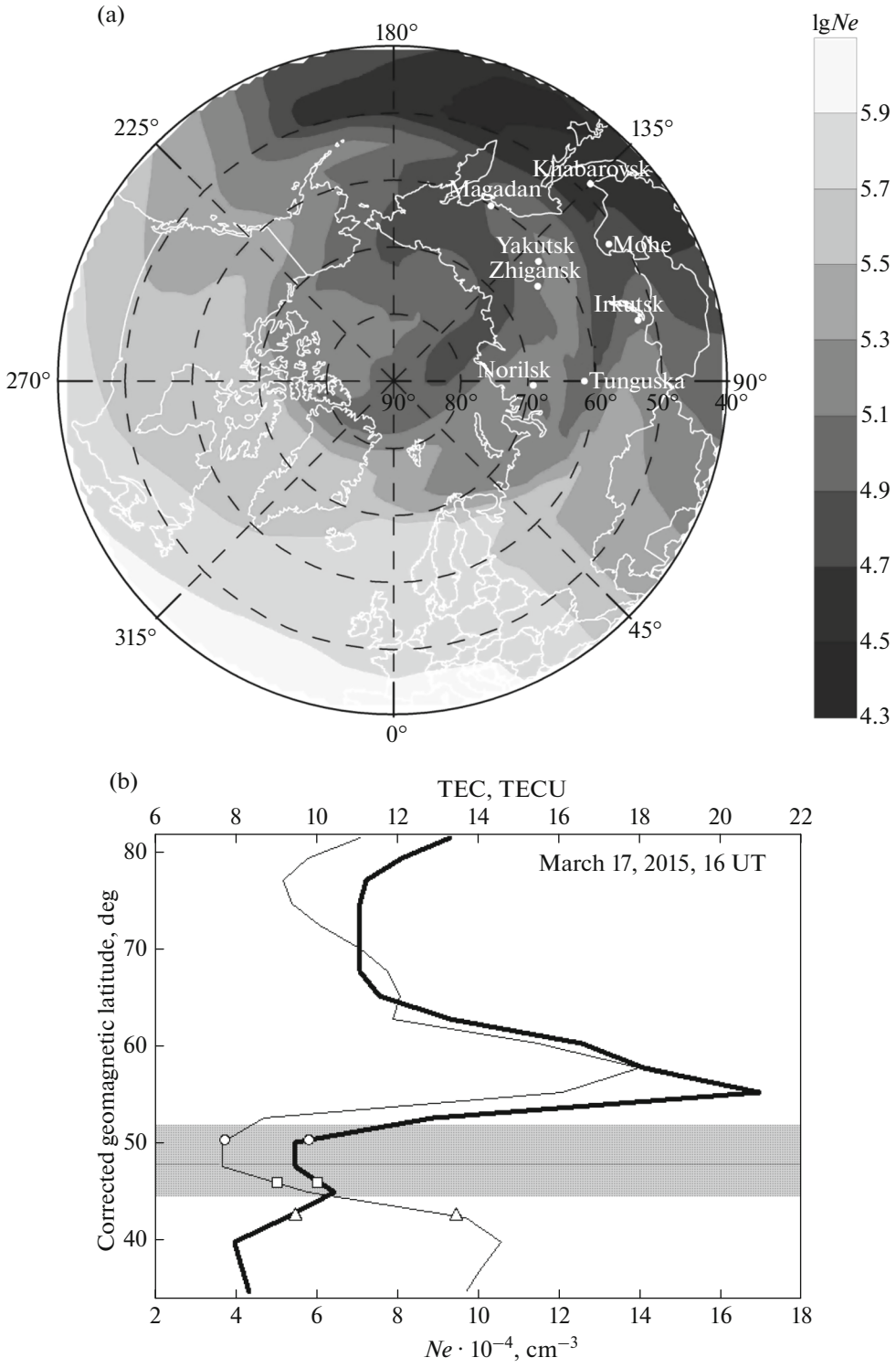

Fig. 8. (a) Electron density distribution at a height of 300 km, calculated for 1600 UT on March 17, 2015, and (b) latitudinal course of TEC (thin line) and maximum electron density *Ne* (bold line) according to calculations (Tashchilin and Romanova, 2014).

thermosphere and the flux of solar ionizing radiation are external parameters of the model. The concentrations of its main components and temperature were determined with the NRLMSISE-00 neutral atmosphere model (Picone et al., 2002). The horizontal wind velocity of thermospheric wind was calculated with the HWM07 model (Drob et al., 2008). The spectrum of solar ionizing radiation was taken from a

model (Richards et al., 1994), and the electric field of magnetospheric convection was calculated from the empirical model (Weimer, 1995).

Figure 8a shows the electron density distribution calculated for 1600 UT of March 17, 2015 (the main phase of the storm). It can be seen that range of low values $foF2 < 2.5$ MHz (which corresponds to lg $Ne <$ 4.9 in Fig. 8a) reached the latitude 52° N. In evening hours, the eastern section of the Magadan–Irkutsk path (from the transmitting point to the midpoint) was near the MIT; therefore, the recorded parameters involved (along with the standard modes) additional diffuse signals with large delays reflected from its polar wall. The northern section of the Norilsk–Irkutsk path was entirely in the precipitation zone. This is confirmed by the recorded values of blanketing *Es* during the main phase of the magnetic storm (see Fig. 3). Because of this, the ionograms of oblique sounding at night hours contain no data due to the absorption in the lower ionosphere.

This shift of the trough to the latitude 52°N is confirmed by data on total electron content (TEC). Figure 8b shows the latitudinal distribution of TEC for 1600 UT on March 17, 2015 (the main phase of the storm). The TEC values were taken from (http://cdaweb.gsfc.nasa.gov/cgi-bin/eval1.cgi), and the values of the maximum of electron density *Ne* were calculated by the model (Tashchilin and Romanova, 2014). The circles, squares, and triangles denote the latitudes of the inner edge of the plasma sheet (Kamide and Winningham, 1977), the MIT minimum according to the model (Deminov et al., 1996a; Deminov et al., 1996b), and MIT minimum according to the model (Zherebtsov et al., 1986), respectively. It can be seen that the range of minimum values of TEC in the latitudinal course (taking into account the scatter of experimental data) coincides with the range of calculated values of electron density.

On the following day (March 18, 2015) at the recovery phase of the storm, the stations of Magadan, Yakutsk, and Tunguska in the evening and night hours of LT were also in the MIT zone, which is confirmed by calculations. It should be noted that phenomena typical for the MIT were observed at Irkutsk earlier during the magnetic storm on October 18–19, 1995 (Zolotukhina et al., 2000).

The third specific feature manifested itself in a sharp decrease in the electron density in comparison with background values in the entire region during the recovery phase of the magnetic storm. As shown in (Danilov and Belik, 1991; Prölss et al., 1991; Buonsanto, 1999; Danilov and Laštovička, 2001), the low daytime $foF2$ values can be caused by changes in the neutral composition of the thermosphere. Due to the heating in the auroral region, the thermospheric gas enriched by molecular ions is transferred by meridional wind to lower latitudes. This leads to the formation of a region of low values of the ratio of concentrations of atomic oxygen to molecular nitrogen $[O]/[N_2]$. According to the GUVI maps (http://guvi.jhuapl.edu/guvi_accessdata.html), the ratio $[O]/[N_2]$ in the given region at a height of 180 km on March 18, 2015, decreased 2–3 times with respect to quiet geomagnetic conditions. The model calculations revealed that $[O]/[N_2] < 1$ during the day at midlatitude stations at a height of 300 km. This led to the appearance of condition *G* on the vertical sounding ionograms, a more than twofold decrease in MOF in daytime hours on March 18, 2015, and a change in the mode composition of propagating HF radiowaves.

6. CONCLUSIONS

(1) On the basis of satellite and ground-based measurement data, we conducted a comprehensive study of heliospheric and magnetospheric parameters, variations in which resulted in the emergence of the magnetic storm of March 17–19, 2015. We revealed a series of processes that determine the distribution of electron density in the ionosphere during the main and recovery phases of the magnetic storm.

(2) In the beginning of the main phase of the magnetic storm, a significant change in the *Bz*-component of the IMF and a rapid change in the field of magnetospheric convection *Ec* led to a shift in the trough boundaries in evening hours of local time to latitudes of 58°–60° N and to the emergence of additional signals propagating beyond the large circle arc over the Magadan–Irkutsk and Norilsk–Irkutsk oblique sounding paths. Ionospheric plasma heating, which resulted from the electric field effect and particle precipitation, caused an increase in the equatorward meridional wind velocity and the upward vertical drift. This served to generate a positive disturbance observed in the vast area under study.

(3) The further strengthening in the field of magnetospheric convection and the western electrojet activity in the second half of the main phase of the storm led to a shift in the MIT boundaries to the equator up to the latitude 52° N. This caused a significant decrease in critical frequencies (<2 MHz) at night and morning hours of local time at midlatitudes. The midlatitude stations of Irkutsk and Mohe recorded sporadic layers conditioned by ionization by precipitating particles. These phenomena are largely typical for the subauroral ionosphere.

(4) In daytime hours during the recovery phase of the storm (March 18, 2015), there was a more than twofold decrease in critical frequencies at all stations and maximum observed frequencies along oblique sounding paths. This decrease in electron density was associated with a significant change in the neutral composition of the atmosphere, which led to increased concentrations of molecular components.

This is responsible for the long-term record of condition *G* at midlatitude stations. The Magadan–Irkutsk and Norilsk–Irkutsk paths were characterized by a changed mode structure of received HF radiowaves.

(5) Analysis of the experimental data obtained at vertical sounding stations and in the network of radio paths, which was confirmed by mathematical calculations, made it possible to obtain new experimental data on the change in ionospheric characteristics and properties of the ionospheric radio channel during magnetic disturbances. These data point to the need for and importance of studies like this under conditions of a disturbed ionosphere and can complement the data obtained earlier on the conditions of propagation of decameter radiowaves over subauroral and midlatitude paths during magnetic storms.

ACKNOWLEDGMENTS

This study was supported by the Russian Foundation for Basic Research, project nos. 13-05-00733, 13-05-00363, and 14-05-00259, and the State Program for the Support of Leading Scientific Schools in Russia of the President of the Russian Federation, project no. NSh-2942.2014.5. The authors are sincerely grateful to the Global Ionospheric Radio Observatory for providing us with vertical sounding ionograms (http://ulcar.uml.edu/DIDBase) and the Russian Heliogeophysical Monitoring Center (RHMC). The authors are also grateful to the personnel of the Kakioka, Honolulu, San Juan, and Hermanus Observatories for promptly providing us with preliminary values of the *Dst*-index for March 2015. The GUVI data were obtained at (http://guvi.jhuapl.edu/guvi_accessdata.html) through the NASA Mission Operations and Data Analysis program.

REFERENCES

Beletskii, A.B., Mikhalev, A.V., Tashchilin, M.A., Kostyleva, N.V., Leonovich, V.A., Podlesnyi, S.V., Syrenova, T.E., Tatarnikov, A.V., and Cherepanov, V.B., Optical observations of midlatitude radiation of the upper atmosphere during the March 17, 2015 magnetic storm, in *Tezisy dokladov Mezhdunarodnogo simpoziuma "Atmosfernaya radiatsiya i dinamika" (MSARD-2015)* (Books of Abstracts of the International Symposium "Atmospheric Radiation and Dynamics" (ISARD-2015)), St. Petersburg: Izd. Sankt-Peterburgskogo gos. univ., 2015, pp. 294–295.

Blagovechshensky, D.V. and Borisova, T.D., Substorm effects of ionosphere and HF propagation, *Radio Sci.*, 2006, vol. 35, no. 5, pp. 1165–1171.

Blagoveshchenskii, D.V. and Zherebtsov, G.A., *Vysokoshirotnye geofizicheskie yavleniya i prognozirovanie korotkovolnovykh kanalov* (High-Latitude Geophysical Phenomena and Prediction of Shortwave Channels), Moscow: Nauka, 1987.

Buonsanto, M.J., Ionospheric storms: A review, *Space Sci. Rev.*, 1999, vol. 88, pp. 563–601.

Burke, W.J., Huang, C.Y., Marcos, F.A., and Wise, J.O., Interplanetary control of thermospheric densities during large magnetic storms, *J. Atmos. Sol.–Terr. Phys.*, 2007, no. 3, pp. 279–287.

Danilov, A.D., The *F*-region response to geomagnetic disturbances (a review), *Geliogeofiz. Issled.*, 2013, no. 5, pp. 1–33.

Danilov, A.D. and Belik, L.D., Thermosphere–ionosphere interaction during magnetic storms, *Geomagn. Aeron.*, 1991, vol. 31, no. 2, pp. 209–222.

Danilov, A.D. and Laštovička, J., Effects of geomagnetic storms on the ionosphere and atmosphere, *Int. J. Geomagn. Aeron.*, 2001, no. 2, pp. 209–224.

Deminov, M.G., Karpachev, A.T., Afonin, V.V., and Annakuliev, S.K., Dynamics of a midlatitude ionospheric trough in the recovery phase of a magnetic storm, *Geomagn. Aeron.* (*Engl. Transl.*), 1996a, vol. 36, no. 4, pp. 452–457.

Deminov, M.G., Karpachev, A.T., Annakuliev, S.K., Afonin, V.V., and Smilauer, Ya., Dynamics of the ionization troughs in the night-time subauroral *F*-region during geomagnetic storms, *Adv. Space Res.*, 1996b, vol. 17, no. 10, pp. 141–145.

Drob, D.P., Emmert, J.T., Crowley, G., et al., An empirical model of the Earth's horizontal wind fields: HWM07, 2008, *J. Geophys. Res.*, vol. 113, A12304. doi 10.1029/2008JA013668

Evlashina, M.L., Mingalev, V.S., Krivilev, V.I., and Mingaleva, G.I., Influence of the nonuniform structure of the high-latitude winter ionosphere on radio wave propagation, *Geomagn. Aeron.*, 1986, vol. 26, no. 5, pp. 747–751.

Gonzalez, W.D., Tsurutani, B.T., Lepping, R.P., and Schwenn, R., Interplanetary phenomena associated with very intense geomagnetic storms, *J. Atmos. Sol.–Terr. Phys.*, 2002, vol. 64, pp. 173–181.

Hajkowicz, L.A. and Hunsucker, R.D., A simultaneous observation of large-scale periodic TIDs in both hemispheres following on onset of auroral disturbances, *Planet. Space Sci.*, 1987, vol. 35, no. 6, pp. 785–791.

Hardy, D.A., Gussenhoven, M.S., Raistrick, R., et al., Statistical and functional representation of the pattern of auroral energy flux, number flux, and conductivity, *J. Geophys. Res.*, 1987, vol. 92, no. A11, pp. 12275–12294.

Ivanov, V.A., Kurkin, V.I., Nosov, V.E., Uryadov, V.P., and Shumaev, V.V., Chirp ionosonde and its application in the ionospheric research, *Radiophys. Quantum Electron.*, 2003, vol. 46, no. 11, pp. 821–851.

Kamide, Y. and Winningham, J.D., A statistical study of the "instantaneous" auroral oval: The equatorial boundary of electron precipitation as observed by the ISIS 1 and 2 satellites, *J. Geophys. Res.*, 1977, vol. 82, no. 35, pp. 5573–5585.

Karpachev, A.T. and Afonin, V.V., Variations in the structure of the high-latitude ionosphere during the March 22–23, 1979, storm based on Cosmos-900 and Intercosmos-19 data, *Geomagn. Aeron. (Engl. Transl.)*, 2004, vol. 44, no. 1, pp. 60–68.

Kurkin, V.I., Matyushonok, S.M., Pirog, O.M., Poddelsky, I.N., Ponomarchuk, S.N., Rozanov, S.V., and Smirnov, V.F., The dynamics of the auroral oval and ionospheric

trough boundaries according to data from DMSP satellites and ground-based ionosonder network, *Adv. Space Res.*, 2006, vol. 38, no. 8, pp. 1772–1777.

Lyons, L.R. and Williams, D.J., *Quantitative Aspects of Magnetospheric Physics*, Dordrecht: D. Reidel, 1984; Moscow: Mir, 1987.

Mendillo, M., Storms in the ionosphere: Patterns and processes for total electron content, *Rev. Geophys.*, 2006, vol. 44, RG4001. doi 10.1029/2005RG000193

Mingalev, V.S., Orlova, M.I., Mingaleva, G.I., and Buyanova, T.V., Modeling of the passage of shortwave radio signals on a high-latitude path under equinox conditions, *Geomagn. Aeron.*, 1990, vol. 30, no. 5, pp. 871–875.

Picone, J.M., Hedin, A.E., Drob, D.P., and Aikin, A.C., NRLMSISE-00 empirical model of the atmosphere: Statistical comparisons and scientific issues, *J. Geophys. Res.*, 2002, vol. 107, no. A12, pp. 1468–1483.

Polekh, N., Ivanova, V., Kurkin, V., Chistyakova, L., and Poddelsky, I., Wave disturbance influence on HF-propagation characteristics, *Adv. Space Res.*, 2010, vol. 46, no. 3, pp. 275–279.

Prölss, G.W. and Ocko, M., Propagation of upper atmosphere storm effect towards lower latitudes, *Adv. Space Res.*, 2000, vol. 26, no. 1, pp. 131–135.

Prölss, G.W., Brace, L.H., Mayr, H.G., Carignan, G.R., Killeen, W.L., and Klobuchar, J.A., Ionospheric storm effects at subauroral latitudes: A case study, *J. Geophys. Res.*, 1991, vol. 96, no. 2, pp. 1275–1288.

Richards, P.G., Fennelly, J.A., and Torr, D.G., EUVAC: Solar EUV flux model for aeronomic calculations, *J. Geophys. Res.*, 1994, vol. 99, no. A5, pp. 8981–8992.

Tashchilin, A.V. and Romanova, E.B., Modeling of properties of the plasmasphere under quiet and disturbed conditions, *Geomagn. Aeron. (Engl. Transl.)*, 2014, vol. 54, no. 1, pp. 11–19.

Warrington, E.M., Stocker, A.J., and Siddle, D.R., Measurement and modeling of HF channel directional spread characteristics for northerly paths, *Radio Sci.*, 2006, vol. 41, RS2006. doi 10.1029/2005RS003294

Weimer, D.R., Models of high-latitude electric potentials derived with a least error fit of spherical harmonic coefficients, *J. Geophys. Res.*, 1995, vol. 100, no. A10, pp. 19595–19607.

Zherebtsov, G.A., Pirog, O.M., and Razuvaev, O.I., The structure and dynamics of the high-latitude ionosphere, *Issled. Geomagn., Aeron. Fiz. Solntsa*, 1986, vol. 76, pp. 165–177.

Zherebtsov, G.A., Kurkin, V.I., Nosov, V.E., Pirog, O.M., Polekh, N.M., and Chistyakova, L.V., Manifestation of ionospheric disturbances in the northeastern region of Russia, *Issled. Geomagn., Aeron. Fiz. Solntsa*, 1997, vol. 107, pp. 10–19.

Zolotukhina, N.A., Polekh, N.M., Rakhmatulin, R.A., and Kharchenko, I.P., Geophysical effects of an interplanetary magnetic cloud on October 18–19, 1995, as deduced from observations at Irkutsk, *J. Atmos. Sol.–Terr. Phys.*, 2000, vol. 62, no. 9, pp. 737–749.

Translated by V. Arutyunyan